Romanian Reports in Physics **71**, 203 (2019)

ENERGY DISTRIBUTION OF EJECTED PHOTOELECTRONS IN $K^{-2}V$ PROCESS

K. I. ISAKOVIĆ, V. M. PETROVIĆ, H. S. DELIBAŠIĆ

University of Kragujevac, Faculty of Science, Department of Physics, Kragujevac, Serbia
E-mail: *kristina_isakovic@yahoo.com*

Received November 29, 2018

Abstract. In the last few years, a great deal of attention has been devoted to Double-Core-Hole states, and especially those involving K-shells, K^{-2} states, as well as, $K^{-2}V$ states, which include simultaneous core ionization and core-excitation. In this paper we gave a theoretical framework that enables prediction of the energy electron distribution in $K^{-2}V$ process in linearly polarized laser field. In order to achieve this, we obtained a formula for the transition rate taking into account the channels of sequential, nonsequential and ionization with ionic core excitation. We started with the $K^{-2}V$ process in helium like atoms. We showed that inclusion of mentioned additional processes significantly influences the transition rate and, at the same time, the energy distribution of the ejected photoelectrons. This is related especially to the energy range of the ejected photoelectrons bringing us to the energy range of low energy electrons which has a significant role in biodamage.

Key words: ionization, excitation, transition rate.

1. INTRODUCTION

Atom and molecule ionization in a strong laser field has been actively studied both theoretically and experimentally long time ago [1, 2]. Extreme laser field intensities allow highly nonlinear processes such as above-threshold ionization, high harmonic generation, Coulomb explosion [3, 4] and, for us especially interesting, laser-induced ionization [5, 6]. Ionization is process in which electrons are removed from any atomic or molecular quantum level and after that they can initiate further excitation [7, 8] or produce secondary electrons by ionization. Photoionization of any multi-electron system usually entails a simultaneous ionization and excitation, while in the most works (papers) only ionization process is observed, and as a consequence the effect of excited states of atoms and ions on the ionization probability has still not been extensively studied. In recent years, S. Corniato *et al.* have been working experimentally on excited states in atoms and molecules [9, 10, 11].

They first developed a theoretical model that provides absolute cross sections for simultaneous core-ionization core-excitation ($K^{-2}V$) and compare its predictions with experimental results [12, 13].

During ionization and excitation processes, the electrons lose a part of their energy, which is important because, today, the main focus is on low energy electrons (LEE), which play a significant role in biodamage [14]. The origin of LEE is most commonly understood to be secondary electrons ionized from core or valence levels by incident radiation and slowed by multiple inelastic scattering events [15], until they become chemically inactive species [16]. This became more evident after a series of recent landmark experiments performed by Sanche and coworkers [17] in Canada.

Because of all mentioned, our intention was to find the energy distribution of the ejected photoelectrons in photoionization processes taking into account both processes, ionization and excitation.

2. THEORETICAL CONCEPTS

Photoionization of atoms and molecules is one of the most fundamental processes of intense laser-matter interactions. It is usually considered as either a multiphoton or a tunneling process depending on the value of the dimensionless Keldysh parameter [18], $\gamma = \omega/\omega_t = \omega\sqrt{2I_p}\,/F$, where ω is the laser frequency, I_p is the unperturbed ionization energy, F is the laser field strength and $\omega_t = F/\sqrt{2I_p}$ is a tunnel frequency. For $\gamma >> 1$ multiphoton ionization is the dominant process, while for $\gamma << 1$ the dominant process is tunnel ionization. Tunneling ionization occurs when the potential barrier of an atom in an intense laser field is deformed in a way that bound electrons can tunnel through this barrier and leave an atom easily.

The atomic system of units $e = m_e = \hbar = 1$ is used throughout this paper [19].

The probability of the classical ionization process can be calculated using the standard formulas of the theory of tunneling ionization such as Keldysh [18], the Perelomov-Popov-Terent'ev (PPT) [20], the Ammosov-Delone-Krainov (ADK) [21] and Smirnov and Chibisov [22]. The ADK formula is one of the most used ones. For the case of non-zero initial momentum, p, it has the following form [21]:

$$W_{ADK} = \frac{F}{8\pi Z}\left(\frac{4eZ^3}{Fn^{*4}}\right)^{2n^*} Exp\left[-\frac{2Z^3}{3Fn^{*3}} - \frac{p^2\gamma^3}{3\omega}\right] \tag{1}$$

where $n^* = Z/\sqrt{2I_p}$ is the effective quantum number and z is the ion charge.

The ADK model was developed based on Dykhne formalism [23]. This approach allows derivation exponentially a small transition rate between the initial bound state i with energy $E_i(t)$ of the considered atomic ion and the final continuum state f with the energy $E_f(t)$:

$$W_{if} \propto \mathrm{Exp}\left[-2\,\mathrm{Im}\,S(\tau)\right] \propto \mathrm{Exp}\left[-2\,\mathrm{Im}\int_0^{\tau}\left(E_f(t)-E_i(t)\right)\mathrm{d}t\right] \tag{2}$$

i.e. the transition rate W_{if} between the initial and the final state is the exponential function of the imaginary part of the action, $S(\tau)$. Here, $E_f(t)$ is the energy of the final state, $E_f(t)=\frac{1}{2}\left[p-\frac{1}{c}\vec{A}(t)\right]^2$, where $\vec{A}(t)$ is the vector potential of the electromagnetic field, $A(t)=-\frac{\omega}{c}F\sin(\omega\tau)$ and τ is the classical turning point [24].

In most papers, the contribution of the excitation process to the rate is neglected. That is why we treated the ionization rate as a cumulative contribution of simultaneous processes, ionization and excitation, as a sequence of events based on which we developed the formula for the transition rate, *i.e.* corresponding the energy distribution formula. We used the Dykhne formalism and applied it to Helium (and helium like) atoms. The photon-impact ionization of the He atom from the $1S(1s^2)$ ground state with excitation of the other remaining electron to the state $2S(2s)$ $(1s\rightarrow 2s)$ or $2P(2p)$ $(1s\rightarrow 2p)$ is the simplest ionization excitation process [25, 13, 26].

We have limited ourselves to a non-relativistic domain. Many recent approaches on field ionization show that there are differences in the ionization rate depending on whether linearly, circularly or elliptically polarized light is used [27]. In this work we considered a linearly polarized laser field.

We started from the initial energy of considered system. Although in atomic or molecular physics it is often a good approximation to assume that the electron–electron correlation plays a minor role, we took it into account through the channels of nonsequential (NSI) ionization [28, 29]. In accordance with this, the initial energy can be written as a sum of the non perturbated ionization energy, I_p, and the term which includes the correlation effect [30]:

$$E_i = I_p + \frac{5Z}{8}\,. \tag{3}$$

Next, we modified the final energy, $E_f(t)$, in way to include the energy of the excitation processes, $E^{\pm} = I_p + J(1s,2s) \pm K(1s,2s)$ [31, 32], as well as the energy of the Coulomb interaction, E_c [20]:

$$E_f = \frac{1}{2}\left[p-\frac{F}{\omega}\sin(\omega\tau)\right]^2 + I_p + J(1s,2s) + K(1s,2s) - E_c\,, \tag{4}$$

where the term $J(1s,2s)$ represents the Coulomb repulsion integrals and $K(1s,2s)$ the exchange integrals [33]. The lower sign between these two terms in Eq. 4

represents the state of lower energy, thus making the configuration 1*s*2*s* of the triplet state lower in energy than the singlet state. For the electron correlation 1*s*,2*s* in the Helium atom, the Coulomb repulsion integral becomes $J(1s,\ 2s) = \frac{17}{81} ZE_h$. The term $K(1s,2s)$ is the quantum exchange integral and for the electron correlation 1*s*,2*s* in the Helium atom is: $K(1s,2s) = \frac{16}{729}\ ZE_h$ [34], where E_h is the energy of a two-electrons atom given by the formula $E_h = \frac{2Z^2}{n^2}$ [35]. In this way, the resultant energy for the final state becomes:

$$E_f = \frac{1}{2}[p - \frac{F}{\omega}\sin(\omega\tau)]^2 + I_p + \frac{17}{81} Z\frac{2Z^2}{n^2} \pm \frac{16}{729} Z\frac{2Z^2}{n^2} - \frac{2n_2 + |m| + 1}{\eta}\sqrt{2I_p}. \quad (5)$$

From the condition for the initial and the final energies in the form: $E_i(\tau) = E_f(\tau)$:

$$p - \frac{F}{\omega}\sin(\omega\tau) = \sqrt{2\left(-2I_p + \frac{5z}{8} - z^3\left(\frac{34}{81} \pm \frac{32}{729}\right) + \frac{2n_2 + |m| + 1}{\eta}\sqrt{2I_p}\right)}, \quad (6)$$

and after some simple transformations and using Maclaurin series, the classical turning point, τ, takes the form:

$$\tau = \frac{p - i\sqrt{2D}}{F} + \frac{\omega^3\left(p - i\sqrt{2D}\right)^3}{6F^3}. \quad (7)$$

In Eq. 7, we introduced the following notation:

$$D = 2I_p - \frac{5Z}{8} + Z^3\left(\frac{34}{81} \pm \frac{32}{729}\right) - \frac{2n_2 + |m| + 1}{\eta}\sqrt{2I_p}.$$

The term D represents some kind of effective energy. Upper sign notes the singlet state in Helium, for which the ionization-excitation process can be observed [33]. Thus, we considered only singlet state of Helium atom. Based on this, we rewrote the previous expression as: $D = 2I_p - \frac{5z}{8} + \frac{z^3}{2} - \frac{2n_2 + |m| + 1}{\eta}\sqrt{2I_p}$.

Now, we calculated the transition rate. Firstly, we substituted Eq. 3 and Eq. 5 into Eq. 2. After that, the action, $S(\tau)$, can be expressed as a sum of four terms:

$$S(\tau) = \int_0^\tau \left[\frac{1}{2}p^2 - \frac{pF}{\omega}\sin(\omega t) + \frac{F^2}{2\omega^2}\sin^2(\omega t) + D\right]\mathrm{d}t. \quad (8)$$

Next, we integrated Eq. 8 over time by parts. Following $W_{if} \propto \mathrm{Exp}[-2\mathrm{Im}S(\tau)]$, after integration, we separated real and imaginary parts. As a result for transition rate W_{if} with cumulative contribution of ionization and excitation processes, we obtained the following formula:

$$W_{iex} \propto \mathrm{Exp}\Big[-2\Big(\sqrt{D}p^2 - \frac{p^2\sqrt{D}}{F} + \frac{D^{5/2}\omega^3}{12F^3} + \frac{5D^{5/2}p^2\omega^3}{12F^3} - \\ - \frac{2D^{3/2}p^2\omega^3}{3F^2} - \frac{2\sqrt{D}p^4\omega^3}{3F^3} + \frac{2\sqrt{D}p^4\omega^3}{3F^2}\Big)\Big] \tag{9}$$

In order to "optimize" the previous expression, we assessed contribution of the initial momentum of ejected photoelectrons. In the limiting case, for a low electron momentum, we supposed that p^2 affects most of the order in comparison to p^4. Also, for a strong field, the terms $\left|\frac{1}{F_0}\right|$ have larger contribution than $\left|\frac{1}{F_0^n}\right|$, $\frac{1}{F_0} \rangle\rangle \frac{1}{F_0^n}\ (n \geq 3)$. Additionally, we introduced the effective Keldysh parameter $\gamma^* = \omega\sqrt{2D}/F$, as well as the new effective quantum number $n^{**} = Z/\sqrt{2D}$. Bearing all this in mind follows that the transition rate in a monochromatic, linearly polarized laser field from excited states of the helium atom can be rewritten as:

$$W_{iex}(p) \propto \mathrm{Exp}\left[-\frac{Z^3\omega\gamma^{*2}}{6Fn^{**3}} - \frac{2p^2Z}{n^{**}}\left(1 - \frac{2\gamma^2}{3}\right)\right] \tag{10}$$

According to Eq. 10 the transition rate depends on the square degrees of the initial momentum p of the ejected photoelectrons, as well as the introduced effective Keldysh parameter, γ^*, and the new effective quantum number, n^{**}.

Next, we applied this result in order to express the non-relativistic energy distribution of ejected photoelectrons in the linearly polarized laser field. If a system's total energy is independent of the coordinate η then momentum is conserved along the classical path *i.e.* $p_\eta = p$ for small angles [24], so combining equation $W(p) = W(0)\,\mathrm{Exp}\left[-\frac{p^2\omega^2\left(2I_p\right)^{3/2}}{3F^2}\right]$ with the well known expressions for $E = \frac{p_{\mathrm{II}}^2}{2}$ [36] it follows that the energetic distribution of the ejected photoelectrons may be written as:

$$W_{iex}(E) \propto \mathrm{Exp}\left[-\frac{Z^3\omega\gamma^{*2}}{6Fn^{**3}} - \frac{4EZ}{n^{**}}\left(1 - \frac{2\gamma^2}{3}\right)\right]\mathrm{Exp}\left[-\frac{2E\omega^2\left(2I_p\right)^{3/2}}{3F^3}\right] \tag{11}$$

Equation 11 presents the formula for a electron energy distribution. It describes the exponential dependence of the energy distribution on the amplitude of the laser field, unperturbated ionization potential, as well as effective Keldysh parameter, γ^*, and the new effective quantum number, n^{**}. Additional terms, which can be seen in the formula, compared to the standard ADK formula [21], are directly related to the electron excitation.

3. DISCUSSION OF RESULTS

Furthermore, we applied our formula on a single ionized helium atom, He^+, in a linearly polarized laser field, $\lambda = 10.6\,\mu\text{m}$ ($\omega = 0.004298$ a.u.). We assumed short pulses (there is no ponderomotive force) and the general laser beam shape. As we said, our intention was to discuss the influence of different ionization channels on the transition rate. To achieve this we compared our results with those obtained using the standard ADK formula [21].

In Fig. 1 we gave comparative review of the theoretical curves, obtained based on the ADK formula, $W_{ADK}(p)$ (left plot), Eq. 1 where only ionization process is observed and our formula, $W_{iex}(p)$ (right plot), Eq. 10 with cumulative contribution of ionization and excitation processes.

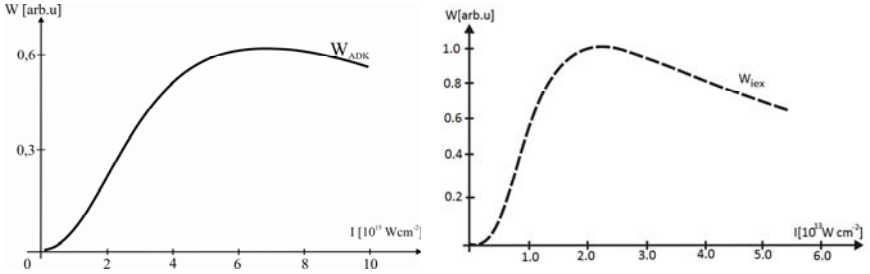

Fig. 1 – Comparative review of the transition rate of a) the ADK theory, $W_{ADK}(p)$ as a function of the laser field intensity $I = 10^{15} - 10^{16}$ Wcm^{-2} and b) $W_{iex}(p)$, as a function of the laser field intensity $I = 10^{13} - 6\times10^{13}$ Wcm^{-2}. The parabolic coordinate is set on $\eta = 14$. The initial momentum, $p \neq 0$.

Both calculated theoretical curves are presented as a function of the laser field intensity, but there are changes in their slopes which shows influence of the additional ionization channels on the average behavior of the rate, *i.e.* the curves behave qualitatively differently. The standard theoretical ADK curve (Fig. 1, left plot), increases rapidly with field increasing, reaches a maximal value and then decreases slowly. The presence of the saturation effect around the field intensity $I \sim 6 \times 10^{15}$ Wcm^{-2} is evident [37, 38]. The curve, obtained based on our formula (Fig. 1, right plot) after the short range of the rapid increase reaches maximum on $I \sim 3 \times 10^{13}$ Wcm^{-2}. Than the graph shows considerably faster rate declination

(compared to $W_{ADK}(p)$) for some definite laser field intensity interval. Both curves generally have asymmetric form with respect to the field intensity on which the maximal value is achieved. We would like to note that, for the same conditions, the $W_{iex}(p)$ curve is shifted to lower field intensity. Also it can be seen that the ADK transition rate $W_{ADK}(p)$ is lower compared to $W_{iex}(p)$. The shift to lower intensities "put" the ejected photoelectrons in the range of LEE, which is in accordance with [39] and [40] who showed that ion yield data are shifted down in intensity compared to ADK theory. Additionally, we compared our results with experimental data obtained by [39, 41] and concluded that our curve (Fig. 1, right plot) has the characteristic "flow" which can be seen in [39, 42].

Our analysis shows that the $W_{iex}(p)$ is very sensitive on field intensity, as well as the parabolic coordinate η. The minimal change of those parameters strongly affects the rate. In order to illustrate the dependence of the ionization excitation transition rate $W_{iex}(p)$ to the parabolic coordinate, η, and laser field intensity, I, in Fig. 2 (3D graph) we showed the behavior of $W_{iex}(p)$ with the short range of laser field intensity and parabolic coordinate.

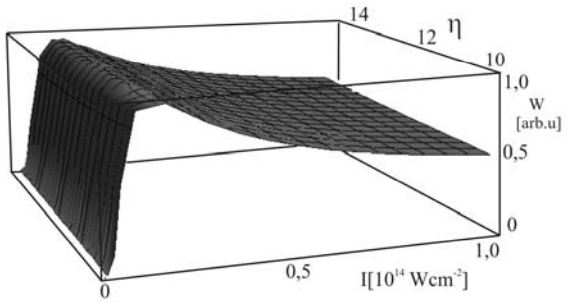

Fig. 2 – 3D graph for the $W_{iex}(p)$ as a function of the parabolic coordinate $\eta = 10 - 14$ and the field intensity $I = 10^{13} - 10^{14}$ Wcm^{-2}.

Next, we observed the energy distribution spectrum, $W_{iex}(E)$, of obtained photoelectrons during the photoionization process. We were motivated by idea that our theoretical research in the field of ionization processes could be linked to biomolecules and, further to biodamage. In order to present the energy distribution, we transformed the intensity axis into units of energy. In a limited case, the energy shift of the continuum is equal to the ponderomotive energy, the cycle averaged kinetic energy of an electron in a laser field, $\Delta E_\infty = U_p$. For a peak intensity, I, in Wcm^{-2} and wavelength, λ in μm, the ponderomotive energy can be estimated in electron volts (eV) using the relation $U_p = 9.33 \times 10^{-14} I\lambda^2$ [43]. Now, we can observe the energy distribution of the ejected photoelectrons and discuss it.

In Fig. 3, we compared the energy distribution of ejected photoelectrons obtained based on the ADK, $W_{ADK}(E)$, (left plot), and our formula, $W_{iex}(E)$, (right plot), on the field intensity range $I = 10^{13} - 10^{14}$ Wcm^{-2}.

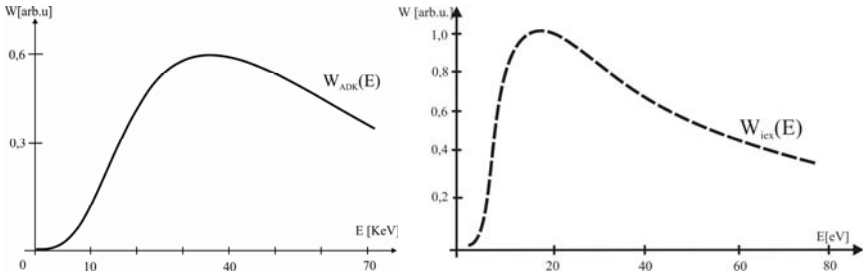

Fig. 3 – Comparative review of the energy distribution:
a) $W_{ADK}(E)$; b) $W_{iex}(E)$ as a function of the energy.

From Fig. 3 is obvious that the difference between theoretical curves exists. Both curves on some definite intensity range increase, reach the maximum (more or less defined) and then approach to energy axis but with different asymptotic slopes. Lower then the laser intensity $I \sim 3 \times 10^{13}$ Wcm^{-2}, *i.e.* energy $E \sim 22$ eV, it can be seen that $W_{iex}(E)$ increases very rapidly with increasing laser field energy. The obtained results, compared to $W_{ADK}(E)$, show that the simultaneous ionization excitation distribution, $W_{iex}(E)$, definitely enhances over the entire energy range. Also, from Fig. 3 it can be seen that the width of $W_{iex}(E)$ is narrower, with a relatively defined maximum on $E \sim 22$ eV. It follows that the inclusion of the excitation process into the observation of the photoionization process is important and shifts the electron energy into the range of LEE, that is in accordance with [44]. Obtained energy range is in agreement with [45] and almost perfect with [46, 42] and [47] who obtained exactly the same energy range of the photoelectron energy distribution in the tunneling regime. Also, the entire photoelectron energy distribution curve exhibits the well-documented and expected behaviour [42, 47].

Finally, based on all aforementioned, we concluded that our results, for the energy distribution of ejected photoelectrons, show better agreement with the experimental data than those calculated based on the standard ADK [21]. The differences lie in the treatment of the "fast" electron and in the details of the wavefunctions for the initial bound state and the continuum states.

Similar results are obtained for wavelength of 800 nm produced by a titanium: sapphire-based laser system $\lambda = 800$ nm ($\omega = 0.05696$ a.u.) and for the other noble atoms.

4. CONCLUSION

In conclusion, a formula for the ionization-excitation transition rate has been developed. Unlike the ADK theory, our formula takes into account simultaneous ionization excitation processes. Based on the obtained results, we concluded that it is important to include additional mechanisms in the observation of the photoionization

process. Also, we gave comparative review of the transition rate's theoretical curves for standard ADK and our formula. Our results show the definite enhancement of the simultaneous ionization excitation rate and the shift to lower energy range.

The obtained results can serve as guidance for experiments in order to determine the intensity range in which LEE can be expected. Our intention, in further work, is to expand our research to more complex atom systems, as well as to molecules, in order to determine fundamental mechanisms that are involved in processes in biomolecules, but also, based on the theoretical model, to find the controlling mechanisms of relevant parameters and at the same time, induced effects.

Acknowledgments. The authors are grateful to the Serbian Ministry of Education, Science and Technological Development for financial support through Project 171020. Help from the COST CM 1204 project, the XLIC action, XUV/X-ray light and fast ions for ultrafast chemistry, is also highly acknowledged.

REFERENCES

1. V. M. Rylyuk, *Strong-field atomic ionization in an elliptically polarized laser field and a constant magnetic field*, Phys. Rev. A **93**, 053404 (2016).
2. A. Hartung, F. Morales, M. Kunitski et al., *Electron spin polarization in strong-field ionization of xenon atoms*, Nature Photonics **10**, 526–528 (2016).
3. A. Becker, F.H. Faisal, *S-matrix analysis of ionization yields of noble gas atoms at the focus of Ti: sapphire laser pulses*, Journal of Physics B: Atomic, Molecular and Optical Physics **32**, L335 (1999).
4. M. Gajda, J. Krzywinski, L. Plucinski, B. Piraux, *Interaction of a hydrogen atom with an intense pulse of vacuum ultraviolet radiation*, Journal of Physics B: Atomic, Molecular and Optical Physics **33**(6), 1271 (2000).
5. P. R. Della, J. Fiol, P.D. Fainstein, *Laser-induced ionization of simple atoms and molecular ions*, Journal of Physics: Conference Series **388**(3), 032048 (2012).
6. P. L. Knight, M. A. Lauder, B. J. Dalton, *Laser-induced continuum structure*, Physics Reports **190**(1), 1–61 (1990).
7. A. Chaudhry, H. Kleinpoppen, *Experimental Techniques, In Analysis of Excitation and Ionization of Atoms and Molecules by Electron Impact*, Springer, New York, 2011, pp. 107–137.
8. IUPAC: *Compendium of Chemical Terminology*, 2nd ed. ("Gold Book") 1997. Online corrected version: (2006–) "Ionization".
9. S. Carniato, P. Selles, L. Andric et al., *Single photon simultaneous K-shell ionization and K-shell excitation. I. Theoretical model applied to the interpretation of experimental results on H_2O*. The Journal of Chemical Physics **142**, 014308 (2015a).
10. S. Carniato, P. Selles, L. Andric et al., *Single photon simultaneous K-shell ionization and K-shell excitation. II. Specificities of hollow nitrogen molecular ions*, The Journal of Chemical Physics **142**(1), 014307 (2015b).
11. S. Carniato, P. Selles, P. Lablanquie et al., *Photon-energy dependence of single-photon simultaneous core ionization and core excitation in CO_2*, Phys. Rev. A **94**, 013416 (2016).
12. M. Nakano, P. Selles, P. Lablanquie et al., *Near-Edge X-Ray Absorption Fine Structures Revealed in Core Ionization Photoelectron Spectroscopy*, Physical Review Letters **111**(12), 123001 (2013).
13. G. Goldsztejn, T. Marchenko, R. Püttner et al., *Double-Core-Hole States in Neon: Lifetime, Post-Collision Interaction, and Spectral Assignmen,* Physical Review Letters **117**(13), 133001 (2016).
14. L. Sanche, *Low energy electron-driven damage in biomolecules*, L. Eur. Phys. J. D **35**, 367–390 (2005).

15. M. Mucke, M. Braune, S. Barth et al., *A hitherto unrecognized source of low-energy electrons in water*, Nature Physics **6**, 143–146 (2010).
16. L. Sanche, T.D. Märk, Y. Hatano, *Atomic and Molecular Data for Radiotherapy and Radiation Research*, IAEA TECDOC **799**, 274–329 (1995).
17. B. Boudaïffa, P. Cloutier, D. Hunting et al., *Resonant formation of DNA strand breaks by low-energy (3 to 20 eV) electrons*, Science **287**, 1658–60 (2000)
18. L. V. Keldysh, *Ionization in the field of a strong electromagnetic wave*, Sov. Phys. JETP **20**, 1307–1314 (1965).
19. R. McWeeny, *Natural Units in Atomic and Molecular Physics*, Nature **243**, 196–198 (1973).
20. A.M. Perelomov, V.S. Popov, M.V. Terent'ec, *Ionization of Atoms in an Alternating Electric Field*, Sov. Phys. JETP **23**, 924–934 (1966).
21. M.V. Ammosov, N.B. Delone, V.P. Krainov, *Tunnel ionization of complex atoms and of atomic ions in an alternating electromagnetic field*, Sov. Phys. JETP **64**, 1191–1194 (1986).
22. B.M. Smirnov, M.I Chibisov*, The Breaking Up of Atomic Particles by an Electric Field and by Electron Collisions*, Sov. Phys. JETP **22**, 585–592 (1966).
23. A. M. Dykhne, *Adiabatic perturbation of states of the discrete spectrum*, Zh. Éksp. Teor. Fiz. **41**, 1324 (1961).
24. L.D. Landau, E. M. Lifshitz, *Quantum Mechanics: Non-Relativistic Theory*, 3rd ed. Pergamon, Oxford, p. 298, 1991.
25. S.-Y. Sun, X.-F. Jia, *(e, 2e) Investigations of the Simultaneous Ionization and Excitation of Helium to He+(n=2)*, Chin. J. Chem. Phys. **26**, 576–579 (2013).
26. F. Penent, S. Carniato, P. Lablanquie et al., *Single photon core ionization with core excitation: a new spectroscopic tool*, Phys.: Conf. Ser. **635**, 112093 (2015).
27. N.B. Delone, V. P. Krainov, *Tunneling and barrier-suppression ionization of atoms and ions in a laser radiation field*, Phys.-Usp. **41** 469–485 (1998).
28. R. Moshammer, Y. H. Jiang, L. Foucar et al., *Few-Photon Multiple Ionization of Ne and Ar by Strong Free-Electron-Laser Pulses*, Phys. Rev. Lett. **98**, 203001 (2007).
29. V.M. Petrović, T.B. Miladinović, *Effect of Electron-Electron Correlation on the Nonsequential Ionization Process in a Linearly Polarized Laser Field*, Rom. J. Phys. **62**, 202 (2017).
30. V. P. Krainov, *High-energy electron spectra of atoms undergoing direct tunnelling ionization by linearly polarized laser radiation*, J. Phys. B: At. Mol. Opt. Phys. **36**, 169–172 (2003).
31. P. Sancho, L. Plaja, *Metastable superpositions of ortho- and para-Helium states*, Physics Letters A **372**, 5560–5563 (2008).
32. M. Inguscio, L. Fallani, *Atomic Physics: Precise Measurements and Ultracold Matter*, OUP Oxford, first edition, p. 125, 2013.
33. P. Atkins, R. Friedman, *Physical Chemistry*, 4th Edition, W. H. Freeman and Company, New York, 2005, p. 235.
34. A. Hutem, S. Boonchui, *Evaluation of Coulomb and exchange integrals for higher excited states of helium atom by using spherical harmonics series*, J. Math. Chem. **50**, 2086–2102 (2012).
35. G. Tanner, K. Richter, J.M. Rost, *The theory of two-electron atoms: between ground state and complete fragmentation*, Rev. Mod. Phys. **72**, 497 (2000).
36. N. B. Delone, I. Yu. Kiyan, V. P. Krainov, *Ionization of atoms by a strong low-frequency field*, Laser Phys. **3**, 312–322 (1993).
37. L.F. DiMauro, B. Sheehy, B. Walker et al., *Atomic Electron Correlations in Intense Laser Fields*, AIP Conf. Proc., **477**, 386–399 (1998).
38. M. Petersilka, E. K. U. Gross, *Strong-Field Double Ionization of Helium: A Density-Functional Perspective*, Laser Physics **9**, 1–10 (1999).
39. S. J. B. Corrigan, A. von Engel, *The Excitation of Helium by Electrons of Low Energy*, Proc. Phys. Soc. **72**, 786–790 (1958).
40. D.N. Fittinghoff, P.R. Bolton, B. Chang, K.C. Kulander, *Observation of nonsequential double ionization of helium with optical tunneling*, Physical Review Letters **69**, 2642 (1992).

41. J. O. P. Pedersen, F. Folkmann, *Simultaneous excitation and ionization of helium by fast projectiles*, J. Phys. B: At. Mol. Opt. Phys. **23**, 441–456 (1990).
42. C. I. Blaga, F. Catoire, P. Colosimo et al., *Strong-field photoionization revisited,* Nature Physics, 5, Nature Publishing Group, 2009.
43. E. Sistrunk, *Scaled strong field interactions at long wavelengths*, Ph.D Dissertation, The Ohio State University, 2011.
44. R. Lafon, J. L. Chaloupka, B. Sheehy et al., *Electron Energy Spectra From Intense Laser Double Ionization of Helium*, Phys. Rev. Lett. **86**, 2762–2765 (2001).
45. G. Franz, *Low Pressure Plasmas and Microstructuring Technology*, Springer, p. 13, 2009.
46. L. Avaldi, R. Camilloni, R. Multari et al., *Absolute measurements of ionization-excitation of helium at intermediate energies and their interpretation*. Journal of Physics B: Atomic, Molecular and Optical Physics **31**, 2981–2997 (1998).
47. D. M. Goebel, I. Katz, *Fundamentals of Electric Propulsion: Ion and Hall Thrusters*, A John Wiley & Sons, Inc., Hoboken, New Jersey, 2008, p. 472.